Ph.D. Thesis

MODULATION OF THE PRIMARY QUINONE ENERGETICS IN REACTION CENTERS OF PHOTOSYNTHETIC BACTERIA: MUTATION, DELAYED FLUORESCENCE AND MODEL-COMPUTATION

László Rinyu

Project leader: Dr. Péter Maróti, Professor of Biophysics

University of Szeged, Department of Biophysics

Szeged, 2007

1. Introduction

Photosynthesis is one of the basic metabolic processes of the living organisms. Photosynthesizing species (bacteria, algae and higher class plants) convert the energy of light into other forms of free energy (redox potential, electrochemical potential of ions and protons and phosphate-potential) which are directly suitable either to cover the energy need of the vital processes of the cell or to storage. The ultimate free energy of the photosynthetic organisms is the radiation of the sun that serves as energy source not only for themselves, but, indirectly, for other living organisms (e.g. animals and human mankind), as well. Thus, the photosynthetic species supply the nutrient source for all other living creatures up to the top-predators being at the end of the food chain. Photosynthetic processes can basically be divided into two main categories: light reactions and dark reactions. In the light reactions, sources of the dark reactions are generated (ATP and reduced coenzymes) making possible the production of high-energy carbohydrates via the succession of different biochemical metabolic processes (dark reactions). Light reactions proceed after the absorption of the photon with the contribution of specifically oriented pigments embedded into proteins (pigment-protein complexes). In green plants, where photosynthesis occurs in the most effective way known so far, NADPH and ATP are generated in the course of the light reactions. In this process, two photochemical systems (PSI and PSII) contribute which are well-separated from each other. The water evolving complex connecting to the PSII is uniquely able to decompose the water to protons and molecular oxygen driven indirectly by light. A significant part of the absorbed light energy is stored in the form of proton electrochemical potential that is formed by succession of a series of redox reactions. The transmembrane protonmotive force is the energy source of ATP synthesis. The other part of the absorbed light energy by PSII gets on the PSI completing the process with the absorption of another photon by PSI, resulting in the reduction of the NADP.

The processes of photosynthetic energy conversion in bacteria are considerably more simple than in higher-class green plants. In bacteria, contrary to green plants, only one photochemical system (including the light harvesting antennas and the reaction center protein-pigment complex) operates. As opposed to the linear, partly cyclic electron transport-chain of green plants, the bacterial one is made up of only one cycle, in the course of which the charge couple generated in the reaction center gets stabilized. The reaction center of non-sulfur purple bacteria is similar to the PSII photochemical system of higher plants. Following the absorption of light by the bacteriochlorophyll dimer (P) of the reaction center gets into an excited singlet state (P^*). The energy gap between the ground and the excited states equals to

the energy of the absorbed photon, which is 1380 meV in the case of *Rhodobacter sphareoides* [1]. The carrying of electron from the primary donor to the bacteriopheophytin (Bpheo) is facilitated by the bacteriochlorophyll monomer with the overlapping of the electron clouds of the primary donor and the acceptor bacteriopheophytin. Hereby, the electron gets to the primary quinone by direct tunneling process with the help of the nuclear vibration of the peptide skeleton and the bridging residues (the M252 tryptophan and the M218 methionine [2, 3]). More than 98 % of photon-absorbing reaction centers get into this state, i.e. the quantum-efficiency of photosynthesis is nearly unit. Contrary to this, the energy efficiency of light utilization is much lower, only 30-40 %, as 60-70 % of the energy is lost via the transport of the electron between the cofactors of the protein. The process with the highest energy loss is the reduction of the primary quinone (Q_A). However, this step is important in the irreversible rendering of the charge-separation *in vivo*.

The reaction center of the *Rhodobacter sphaeroides* purple bacteria besides the primary quinone contains another quinone molecule (secondary quinone, Q_B). The two quinones are identical from chemical point of view (both are UQ_{10}), however, they differ in redox and binding properties [4]. It is due to the different protein environment [5]. The primary quinone is located in a strongly hydrophobic environment and one of the protein subunits of the reaction center (H-subunit) isolates it from the aqueous phase. Due to this environment, the quinone is not able to accept a proton after the reduction. Under physiological circumstances, Q_A can be reduced only by one electron, and its doubly reduced form can be observed only at extreme high light intensity and under strongly reducing circumstances [6]. It is able to form several hydrogen bounds with the surrounding amino acids and structure waters, consequently binds to the reaction center very strongly and can be removed only by drastic treatment [7]. Its semiquinone form is rather stable, the free energy change accompanied with the reduction is considerably more positive at the Q_A binding site, than in apolar solvents [8, 9]. The midpoint redox potential of the Q_A/Q_A^- redox couple is influenced not only by the steric and electrostatic interactions with the surrounding proteins, but by the interactions between reaction center-protein and lipid-membrane, as well.

In contrary to the primary quinone, the protein environment of the secondary quinone contains several polar amino acids, whose electric field decreases the energy of the Q_B/Q_B^- redox couple. The quinone form is bound loosely to the reaction center and can be separated easily, or substituted with an inhibitor (e.g. o-phenanthroline, terbutrine, stigmatelline) [10]. Its semiquinone form is also very stable, it has 10^{12} times longer lifetime in the reaction center than in solution [8]. The midpoint redox potential of the Q_B/Q_B^- couple *in vivo* is 60 mV higher than that of the Q_A/Q_A^- couple

at pH 8.0 [11]. The complete reduction of the secondary quinone can proceed in the reaction center: the reduction by two electrons is coupled to uptake of two protons. The generated dihydro-quinol separates from the reaction center protein easily and is replaced by one of the free quinones of the membrane [8, 12].

In addition to the photochemical reaction, the excited dimer can return to the ground state by photon emission, as well. The light emission of the bacterial reaction can occur either by prompt or delayed fluorescence. As both forms of emission originate from P^*, they cannot be separated spectrally. However, their decay times and intensities are significantly different. While the prompt fluorescence decays in a few nanoseconds after the excitation, the delayed fluorescence can be observed in a much more extended time domain due to the slow back reactions (P^+Bpheo^- $\rightarrow P^*Bpheo$, $P^+Q_A^- \rightarrow P^*Q_A$ and $P^+Q_B^- \rightarrow P^*Q_B$) of the precursors [13]. The intensity of the delayed fluorescence is several orders of magnitudes lower than that of the prompt fluorescence. The rate constant of decay of the delayed fluorescence equals to that of the disappearance of the charge-separated state by charge recombination, which proves that the delayed fluorescence originates from leakage type process [14]. Based on the intensity of the delayed fluorescence in the millisecond range relative to that of the prompt fluorescence, the free energy level of the $P^+Q_A^-$ charge-separated state relative to the free energy level of the excited dimer can be determined [15]. This is a special and unique feature of the delayed fluorescence as other methods can hardly give the chance of direct determination of the free energy gap. In addition, the sensitivity of the method based on measurement of delayed fluorescence is surprisingly high. I tried to utilize these advantages of the millisecond delayed fluorescence by systematic modification of several factors that determine the midpoint redox potential of the primary quinone. The application of combined methods (mutation, delayed fluorescence and model calculations) to the primary quinone opened the stage for widespread structural and functional studies of the reaction center protein.

2. Aims

The most important aim of this study was the design and production of reaction center mutants in the binding pocket of the primary quinone to investigate the effect of the amino acids of the protein and lipids of the membrane on the thermodynamics of the primary quinone. The first priority will be the determination of the absolute free energy gap between the P^* and the $P^+Q_A^-$ states in wild type and mutant reaction centers by comparison of the intensities of prompt and delayed fluorescence emitted

by the primary donor of the reaction center. By use of the values of the free energy gaps, I'll determine the in situ midpoint redox potential of the Q_A/Q_A^- redox couple in the mutants.

The reaction center structure with atomic resolution determined by X-ray diffraction study makes possible to calculate the thermodynamic properties of the mutants with computer simulations. Using docking simulations in wild-type and mutant reaction centers, I will calculate the binding free energies of the quinone and semiquinone molecules, and I will estimate the midpoint redox potential of the Q_A/Q_A^- redox couple. Additionally, by use of the free energy perturbation method, I will model the reduction process of the primary quinone molecule in wild-type and mutant reaction centers.

With the application of cardiolipin (diphosphatide-glycerol), as model-lipid I will investigate the interaction between the reaction center protein and the lipid-environment. I'm curious how does it affect the charge-recombination process and how does it influence the free energy level of the charge couple ($P^+Q_A^-$) relative to the energy level of the excited primary donor.

With the investigation of the delayed fluorescence of the reaction center embedded into membrane fragment (chromatophore) I will get further information about the effects of reaction center proteins and lipid membranes on the Q_A. In addition to these studies, I will characterize the complex kinetics of the decay of the delayed fluorescence emitted by chromatophore and special attention will be paid to the fastest kinetic component.

3. Materials and methods

Bacterial strains:

- *Rhodobacter sphaeroides* **R-26** blue-green, carotenoidless strain as wild type,
- *Rhodobacter sphaeroides* **GA** green, carotenoid-containing strain as wild type, and mutant strains are made by site-directed mutations of the Q_A site in GA wild type:
  - **M265IV** $\text{Ile}^{M265} \rightarrow$ Val apolar mutant.
  - **M265IS** $\text{Ile}^{M265} \rightarrow$ Ser polar mutant.
  - **M265IT** $\text{Ile}^{M265} \rightarrow$ Thr polar mutant.
  - **M218MA** $\text{Met}^{M218} \rightarrow$ Ala mutant.
  - **M218MG** $\text{Met}^{M218} \rightarrow$ Gln mutant.

- CYCA1 cytochrome c_2-deficient derivative of *Rhodobacter sphaeroides* 2.4.1 wild-type strain.

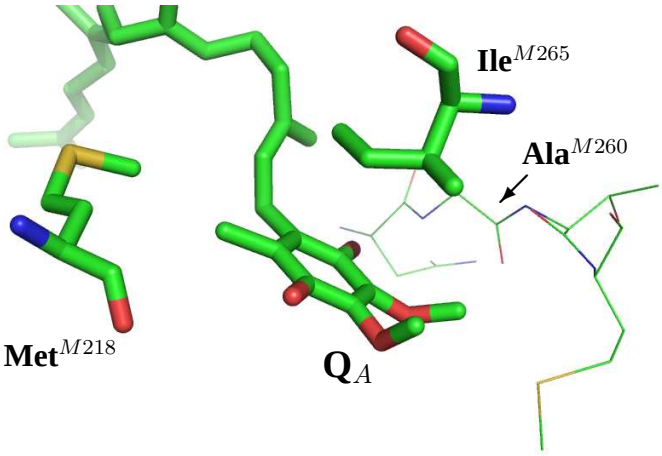

Protein environment of the primary quinone (Q_A) in wild-type reaction centers. Met^{M218} and Ile^{M265} side chains are shown by sticks. The M259-M262 segment is shown by lines. The figure is drawn and rendered by PyMol. The coordinates are from 1AIJ [16] for R26 reaction centers.

Standard protein purification methods were used to isolate the reaction centers of the non-sulfur purple photosynthetic bacteria *Rhodobacter sphaeroides*: the bacterial cells were disrupted by ultrasonic treatment, membrane fragments (chromatophores) were obtained by ultra-centrifugation, and the reaction centers were solubilised by LDAO detergent and ammonium sulfate. The purification of the reaction centers were purified by DEAE-Sephacell ion-exchange chromatography.

The purified mutant reaction centers arrived in frozen state from the group of Prof. Colin A. Wraight (Uversity of Illinois, Biophysics and Plant Biology Center for Biophysics and Computational Biology, Urbana-Champaign, USA).

Measurement of flash-induced absorption change:

The concentration of the reaction center and the charge recombination kinetics were determined from the flash-induced absorption changes of the primer donor (P) at 430 nm and 605 nm in isolated reaction centers and chromatophores, respectively. The measurements were carried out with a homemade single-beam spectrophotometer [17].

Measurement of delayed and prompt fluorescence:

The kinetics of the millisecond delayed fluorescence of the reaction center after single flash excitation was measured with a homemade fluorometer [18]. The major difficulties arose from the extremely low yield of delayed fluorescence (in the range of 10^{-9}), the near-infrared emission wavelength (the maximum of fluorescence is centered at 920 nm), and the intense of the prompt fluorescence emitted during excitation. The reaction center was excited by a frequency-doubled and Q-switched Nd:YAG laser flash (Quantel YG 781-10, wavelength 532 nm, energy 100 mJ and duration 5 ns). The laser beam was introduced into a light-tight box through a green-filter (Schott BG-18). The sample was in a thermostated 1 cm rectangular quartz cuvette selected for extremely low fluorescence ("far UV"; Thermal Syndicate Ltd.). The fluorescence of the reaction center was focused through an infrared cutoff filter (Schott RG-850) onto the photocathode of a red-sensitive photomultiplier (Hamamatsu R-3310-03). Temperature of the sample was measured with K-type (NiCr-Ni) digital thermometer (Vermer VE 305K).

256 and 128 trace of the delayed fluorescence kinetics were averaged in isolated reaction center and chromatophore, respectively. The signals were collected, stored and analyzed with a personal computer.

Calculation of free energy drop from $\mathbf{P^*}$ to $\mathbf{P^+Q_A^-}$:

The free energy gap between P^* and $P^+Q_A^-$ states (ΔG_{P^*A}) was calculated by comparison of the delayed and prompt fluorescence yields according to Arata and Parson [15]. The Q_B binding packet was blocked with inhibitor during experiments. The integral intensities of delayed and prompt fluorescence were measured in the same sample (contained isolated reaction centers) but at very different excitation intensities (both in the linear region) to give similar emission intensities. The integrated intensity of the delayed fluorescence was determined by a one-exponential fit to the decay of the delayed fluorescence signal; the integrated intensity of prompt fluorescence was determined by electronic integration of the prompt fluorescence, using a time constant (1 ms) similar to that of the delayed fluorescence decay time. If the integrated fluorescence intensities were takes as the product of the amplitude

and decay time of fitted curves, we get the following expression:

$$\Delta G_{P^*A} = k_B T \cdot ln(\frac{\phi_f}{k_f \cdot \phi_p} \cdot \frac{A_{\text{kf}} \cdot \tau_{\text{kf}}}{A_p \cdot \tau_p} \cdot t_{\text{filter}}), \quad (1)$$

where k_B is the Boltzmann-constant, T is the temperature, ϕ_f is the prompt fluorescence yield of P^* in reaction centers ($4.0 \pm 1.5 \cdot 10^{-4}$), k_f is the radiative rate constant for reaction center bacteriochlorophyll ($\approx 8 \cdot 10^7 s^{-1}$, from Strickler-Berg relationship [19]), ϕ_p is the quantum yield of charge separation (0.98 ± 0.04), A is the amplitude, τ is the lifetime of the fitted curves, and t_{filter} is the transmission of the glass plate and the gray filter were used in case of prompt fluorescence measurement.

Computer simulations:

The mutant reaction centers were made of employment of 1AIJ structure [16] with mutagenesis module of the PyMol software package [20].

The atomic partial charges of the ubiquinone-4 molecule in states of quinone and semiquinone were determined by Mulliken population analysis, at the level of the semi empirical quantum chemical method AM1 implemented in Mopac93 [21].

Molecular dynamics and free energy perturbation simulations were carried out with Q-package (developed by Johan Åqvist and coworkers) [22].

The docking simulations of the quinone molecules to the reaction center protein were carried out with AutoDock 3.0.5 [23]. The input files were prepared with AutoDockTools software-package.

4. New results

1. The free energy drops from P^* to $P^+Q_A^-$ were determined from the ratio of the intensities of the delayed and prompt fluorescence of bacteriochlorophyll dimer of *Rhodobacter sphaeroides* GA wild-type and Q_A site mutants isolated reaction centers in the physiological pH range. The standard free energy of the primary stable charge pair ($P^+Q_A^-$) relative to that of the excited dimer at pH 8.0 was found to be -890 $\pm$ 5 meV with native ubiquinone-10 as Q_A, in the absence of any secondary quinone, for GA wild-type. (II)

2. M265IV mutant reaction centers exhibited almost unaltered delayed fluorescence, compared to GA wild-type, in the physiological pH range, but with a somewhat flatter pH dependence. The ΔG_{P^*A} was found to be -890 $\pm$ 10 meV

at pH 8.0 for M265IV mutant reaction centers, which was in a good agreement whit the value of GA wild-type at the same pH. At pH 10.5, ΔG_{P^*A} for M265IV reactions centers was 20 meV more negative than for GA wild-type reaction centers, because of the different pH dependency. (II)

3. The two M265 polar mutants (M265IS and M265IT) gave substantially higher delayed fluorescence emission intensity than GA wild-type reaction centers at the physiological pH range, indicating a much smaller energy gap between P^* and $P^+Q_A^-$. The ΔG_{P^*A} was found to be -830 $\pm$ 10 meV for M265IS and -775 $\pm$ 5 meV for M265IT at pH 8.0. Compared to wild-type reaction centers, these values correspond to shifts in the midpoint redox potential (E_m) of Q_A of -60 mV and -115 mV, respectively.
   Based on the available data of reaction center structures and the former FTIR studies, the following explanation is given to this phenomena: The substantial change in E_m of Q_A seen in the polar M265 mutants arises from subtle changes in the length of the hydrogen bonds from quinone environment to quinone carbonyls. It was proposed that the hydroxyl group of serine and threonine side chains is hydrogen bonded to the peptid carbonyl of Thr^{M261}, pushing away the extended backbone region of M259-M262. The Ala^{M260} also moves away from the primary quinone, which residue resides within hydrogen bond length from Q_A in wild-type reaction centers. The transformed environment and the rearrangement of hydrogen bonds (which is stabilized the quinone) were caused the altering of the redox properties of the primary quinone. (II)

4. The M218MA and the M218MG mutants also gave substantially higher delayed fluorescence emission intensity than wild-type reaction centers at the physiological pH range. The ΔG_{P^*A} was found to be -835 $\pm$ 20 meV for M218MA and -805 $\pm$ 10 meV for M218MG at pH 8.0. These values indicate E_m shifts for Q_A of -55 mV and -85 mV, respectively. Both M218 mutants showed qualitatively similar pH dependencies to those of GA wild-type and the M265 mutants.
   In the absence of a secondary donor to re-reduced P^+, back reaction of the charge-separated state, $P^+Q_A^-$, was monitored as P recovery at 430 nm. In wild-type reaction centers, the apparent rate constant (k_P^A) is about 9 s^{-1}, at room temperature. In both M218 mutants this rate was accelerated: k_P^A = 27 s^{-1} for M218MA, and k_P^A = 38 s^{-1} for M218MG. In the wild-type, with ubiquinone-10 as Q_A, the recombination process is by direct tunneling from Q_A^- to P^+ [24]. However, as the redox potential of Q_A is lowered, e.g., by

mutation, a thermally activated route via P^+Bpheo^- becomes accessible. The accelerated back reaction process is the unambiguous sign that the thermally activated route turns on.
The structural basis for the substantial effect of the M218 mutations is not known at this time. The substituted residues, alanine and glycine, are very much smaller than the native methionine, which closes off one side of the Q_A pocket and contributes to the packing between Q_A and $Bpheo_A$. Beside the methionine the Thr^{M252} also acts as a direct tunneling route to the Q_A for electrons to reduce the primary quinone [2, 3]. It is possible that the small side chain volume of the mutant residues allows sequestration of one or more water molecules close to the quinone. The E_m shifts in these mutants with anthraquinone as Q_A is significantly smaller than for the native ubiquinone (basis on recombination kinetics measurements). This might indicate that the large anthraquinone moiety fills more of the available space than does ubiquinone. (II)

5. Addition of cardiolipin to isolated reaction centers in detergent suspension caused a significant slowing of the back reaction (charge recombination) of $P^+Q_B^-$. The effect showed half saturation at about 10 - 20 μM cardiolipin. Since the major route for recombination is via the $P^+Q_A^-$ state [25, 26, 27], this is indicative of a large equilibrium constant for the one electron transfer, $Q_A^-Q_B \leftarrow Q_AQ_B^-$. With 100 μM cardiolipin, at pH 8.0, the slowing was approximately 3-fold, consistent with a 30 meV increase in the free energy drop from Q_A^- to Q_B. The effect was constant across the pH range, from pH 6 to 10.5. The relative amplitude of the slow phase of the back reaction also increased from 70 % to >90 % in the presence of cardiolipin, indicating a substantial increase in the functional occupancy of the Q_B site.
The intensity of delayed fluorescence from wild-type reaction centers with inhibited by terbutrin, was increased 5 - 7-fold in the presence of cardiolipin. Comparison of the integrated intensities showed the magnitude of ΔG_{P^*A} to decrease by 30 $\pm$ 10 meV. The increased delayed fluorescence yield from $P^+Q_A^-$ and slowing of the $P^+Q_B^-$ back reaction by low levels of cardiolipin show that this lipid lowers the E_m of Q_A by 30 - 40 mV. (II)

6. Upon identical reaction center concentrations in chromatophore and in detergent suspension, the intensity of the delayed fluorescence is two order of magnitudes higher in chromatophore than in micelles. The possible reason of this behaviour is the different environment of the reaction centers in the two media. The protein in micellar solution forms weak interactions with the disor-

dered detergent molecules. On the other hand in membrane fragments, the interaction between the reaction center protein and the lipid molecules becomes dominant and shifts the midpoint redox potential of the primary quinone.
We have seen in the previous point, that the mutation of the Q_A site residues caused significant shifts in the midpoint redox potential of the Q_A/Q_A^- redox couple. If this shifts occurs to the negative directions, the delayed fluorescence intensity increases exponentially. We found the same effect in case of interaction of the cardiolipin molecules and reaction centers, which was a good approach of the native membrane environment. Based on numerous similar experiments, the native membrane could shift the midpoint redox potential of the Q_A/Q_A^- redox couple by 100 mV to negative direction compared to detergent suspension. I draw the conclusion from these facts that the interaction between the redox center of the reaction centers and the native membrane lipids is one of the major factors which caused the observed change in delayed fluorescence intensity.

7. I observed that the delayed fluorescence intensity decreased by one-two orders of magnitudes, while the prompt fluorescence intensity increased 2-3-fold during titration of zwitterionic detergent (LDAO) to chromatophore. In chromatophore, in contrast to isolated reaction centers, there is tight cooperation between the light harvesting systems and the reaction center protein in addition to the reaction center-membrane-lipid interaction. While in isolated reaction centers the delayed fluorescence originates from the bacteriochlorophyll dimer, in chromatophore the precursor of the delayed fluorescence can be an antenna bacteriochlorophyll, as well. Here the P^* state (which is formed during the back reaction) may delocalize in the antenna complex via very efficient the energy-(exciton) transfer from the reaction centers. If this occurs then the photon is emitted by one of the antenna-pigments, and the emission yield can be different from that of the dimer in the reaction center.
The increase of the concentration of the LDAO causes the weakening of the cooperation between reaction centers and antenna-system and can finally break it up. The experimental results show that the yield of the fluorescence depends on the location of disappearance (deactivation) of the electron excited state (exciton): it can happen either in the bacterioclorophyll dimer of the reaction center or in the antenna system. Based on the LDAO titration experiments, the yield of the fluorescence in the antenna system is smaller than in the dimer of the reaction centers.

8. Upon inhibition of the electron transfer between the Q_A and Q_B, I found a new

and fast (lifetime $\approx$ 10 ms) component in the milliseconds delayed fluorescence kinetics of chromatophore, in addition to the slow component (lifetime $\approx$ 100 ms), which represents the $P^+Q_A^- \rightarrow PQ_A$ back reaction. I could not find component of equivalent lifetime neither in absorption change kinetics of oxidized dimer, nor in millisecond delayed fluorescence kinetics of isolated reaction centers. The simplest explanation of this new component could be related to the not complete relaxation of the $P^+Q_A^-$ state in the (sub)millisecond time range. I argue for a hot transient state (it is not relaxed) of the charge separated state ($P^+Q_A^-$) and the protein environment. The relaxation of this transient state needs long time. The reason why we can not make distinction between the two components in absorption is that the relaxed and unrelaxed states both belong to the same redox state. Thus, the hot transient state is "silent" in absorption kinetics, but not in delayed fluorescence kinetics.
The fast and the slow components of delayed fluorescence behave similarly under numerous treatments. The free energies of the two states showed similar dependency on pH, detergent (LDAO) concentration, actual redox potential or concentration of external electron donors (ferrocene and TMPD). The similar behaviour to these treatments indicates that the two components might have common origin, i.e. they reflect the same redox state but different vibrational state of the primary charge pair. The latter property is supported by the different temperature dependence of the components. The van't Hoff plots of the different components reveals that the process is entropy- and enthalpy-driven in the fast and slow component, respectively: small enthalpy-change ($\Delta H \approx$ 45 meV) describes the back reaction from the non-relaxated $P^+Q_A^-$ state to the P^* electron excited state, while the same process needs much larger enthalpy-change ($\Delta H \approx$ 620 meV) from the relaxed $P^+Q_A^-$ state. Because the free energy levels of the two states are very close to each other, the difference in enthalpy-change is compensated by entropy-change.

9. By block of the electron transfer between $Q_A^-Q_B$ and $Q_AQ_B^-$ with an inhibitor, the population of $P^+Q_A^-$ charge separated state and therefore the intensity of delayed fluorescence will increase. Stigmatellin and terbutrin inhibitors tested on chromatophores at neutral pH (pH = 7.0) were found to act similarly. The effect could be saturated by high enough concentrations.
In contrast, at alkaline pH (pH = 10.0) the inhibitors showed different behaviour: the effect of terbutrin could be saturated but stigmatelline (even at high concentrations as 50 μM) not. For reaction centers solubilized in detergent, this large different was not present. To explain this behaviour, we have

to assume special interactions of reaction centers with its surroundings. The interactions can deform the geometry of the secondary quinone binding site at high pH values leading to break of hydrogen bridge bonds that have important role in stabilization of the inhibitor (e.g. stigmatellin). This process can result in efficient decrease of binding affinity and can cause the observed loss of activity of the inhibitor. (III)

10. The atomic partial charges of the ubiquinone-4 molecule were determined in two redox states (quinone and semiquinone) by Mulliken population analysis, at the level of the semi empirical quantum chemical method AM1 implemented in Mopac93 [21]. The atomic partial charges relate to the geometry of the ubiquinone molecule is described in the 1AIJ structure [16]. The determined charges were used in the subsequently simulations. (I)

11. The binding free energies for ubiquinone-4 molecule to primary quinone binding site in reaction center protein was determined by docking simulation in two redox states (quinone and semiquinone) of the quinone. 1AIJ structure [16] was the initial geometry of the wild-type reaction center protein and it was the basis of the construction of the mutants structures.
    The ΔG_{bind} of the quinone state was found to be -13.11 kcal/mol for wild-type which is in the good agreement with the experimental data [28]. The binding free energies were more negative for M265IS, M265IV and M218MG mutants and more positive for M218MA and M265IT mutants than wild-type in case of quinone state. More positive values were expected based on the experimental data. The ΔG_{bind} of the semiquinone state was -15.29 kcal/mol in symmetrical charge distribution for wild-type reaction center and all mutants gave more positive values except of M265IS.
    By use of these binding free energies and the midpoint redox potential of ubiquinone in water solvent (-145 mV [29]), I calculated the shifts of the midpoint redox potential of Q_A/Q_A^- redox couple for mutants reaction centers compared to wild-type. The tendency of these shifts showed partial agreement with the experimental results. The midpoint redox potential of the primary quinone was shifted in positive direction for M218MA and M265IT mutants, and in negative direction for M265IS independently what charge distribution in semiquinone state was used. (IV)

12. The reduction of the primary quinone in reaction center protein was modeled by free energy perturbation method (FEP). The change of the atomic partial charges during the reduction process (quinone gradually turns to semiquinone)

was considered as perturbation. I followed the free energy gap between the two states (Q_A and Q_A^-) in the course of simulation process for different charge distribution of the semiquinone and in case of different types of starting geometry (with or without previous molecular dynamics simulation).
I got the best agreement with experimental data when I used symmetrical charge distribution of semiquinone and the geometries were equilibrated by previous molecular dynamics. In this case the shifts of the midpoint redox potential of the Q_A/Q_A^- redox couple compared to wild-type was the following: M265IS (positive direction), and in the negative direction: M265IV, M218MA and M265IT.
The angle of the methoxy-groups of the quinone molecule changed only in two strains (M265IS and M218MA mutants) during the reduction process. The changes of the angle of C3-O3-C3H_3 methoxy-group were 13 - 15° in both case. Changes were observed also in the number and in the length of the hydrogen bonds formed between the quinone molecule and the protein/water environments during the reduction process. I found, that the reduction process increased the number of the hydrogen bonds and/or decreased the length of the bonds. This behaviour is in fair agreement with the experimental observations, that the state of primary quinone is stabilized by the acceptance of the electron. (IV)

RC type	Atom name		Length [Å]	
	quinone	environment	state	
			quinone	semiquinone
Wild-type	UQA:O2	Thr^{M222}:HG1	3.31	**1.48**
	UQA:O2	Trp^{M252}:HE1	3.33	**2.12**
	UQA:O5	Ala^{M260}:H	3.09	**1.65**
M265IV	UQA:O2	Thr^{M222}:HG1	3.38	**1.77**
	UQA:O2	HOH^{1282}:H2	5.48	**1.79**
	UQA:O5	HOH^{1130}:H2	3.38	**1.65**
M265IS	UQA:O2	His^{M219}:HD1	3.17	**1.77**
	UQA:O2	Thr^{M222}:HG1	**2.48**	**2.16**
	UQA:O2	Trp^{M252}:HE1	3.40	**2.88**
	UQA:O5	Ala^{M260}:H	**2.51**	**1.69**
M265IT	UQA:O2	Thr^{M222}:HG1	**1.82**	**1.50**
	UQA:O2	Trp^{M252}:HE1	**2.68**	3.40
	UQA:O5	Thr^{M265}:HG1	5.42	**1.99**
	UQA:O5	HOH^{1163}:H2	**1.71**	**1.55**
M218MA	UQA:O2	His^{M219}:HD1	4.55	**2.60**
	UQA:O2	Thr^{M222}:HG1	3.31	**1.56**
	UQA:O5	Ala^{M260}:H	**2.65**	**2.50**

The change of the number and/or the length of the hydrogen bonds formed between the primary quinone and the protein/water environment during the FEP simulation, in wild-type and mutants reaction centers. Previous molecular dynamics simulations were carried out on every structure before FEP simulations. The charge distribution of semiquinone was symmetrical.

References

[1] S.C. Straley, W.W. Parson, D.C. Mauzerall, and R.K. Clayton. Pigment content and molar extinction coefficients of photochemical reaction centers from *Rhodopseudomonas spheroides*. *Biochimica et Biophysica Acta - Bioenergetics*, 305(3):597–609, 1973.

[2] T. Kawatsu, T. Kakitani, and T. Yamato. Destructive interference in the electron tunneling through protein media. *J. Phys. Chem. B*, 106(43):11356–11366, 2002.

[3] H. Nishioka, A. Kimura, T. Yamato, T. Kawatsu, and T. Kakitani. Interference, fluctuation, and alternation of electron tunneling in protein media. 1. two tunneling routes in photosynthetic reaction center alternate due to thermal fluctuation of protein conformation. *J. Phys. Chem. B*, 1095(5):1978–1987, 2005.

[4] R.C. Prince, P.L. Dutton, and J.M. Bruce. Electrochemistry of ubiquinones: Menaquinones and plastoquinones in aprotic solvents. *FEBS Letters*, 160(1,2):273–276, 1983.

[5] J.P. Allen, G. Fehér, T.O. Yeates, H. Komiya, and D.C. Rees. Structure of the reaction center from *Rhodobacter sphaeroides* R-26: Protein-cofactor (quinones and Fe^{2+}) interactions. *Proc. Natl. Acad. Sci. USA*, 85:8487–8491, 1988.

[6] M.Y. Okamura, R.A. Isaacson, and G. Fehér. Spectroscopic and kinetic properties of the transient intermediate acceptor in reaction centers of *Rhodopseudomonas sphaeroides*. *Biochimica et Biophysica Acta - Bioenergetics*, 546:394–417, 1979.

[7] M.Y. Okamura, R.A. Isaacson, and G. Fehér. Primary acceptor in bacterial photosynthesis: Obligatory role of ubiquinone in photoactive reaction centers of *Rhodopseudomonas sphaeroides*. *Proc. Natl. Acad. Sci. USA*, 72:3491–3495, 1975.

[8] A.R. Crofts and C.A. Wraight. The electrochemical domain of photosynthesis. *Biochimica et Biophysica Acta - Bioenergetics*, 726:149–185, 1983.

[9] N.W. Woodbury, W.W. Parson, M.R. Gunner, R.C. Prince, and P.L. Dutton. Radical-pair energetics and decay mechanisms in reactionn centers containing anthraquinones, naphtoquinones or benzoquinones in place of ubiquinone. *Biochimica et Biophysica Acta - Bioenergetics*, 851:6–22, 1986.

[10] I. Sinning. Herbicide binding in the bacterial photosynthetic reaction center. *Trends in Biol. Sci.*, 17:150–154, 1992.

[11] A.W. Rutherford and M.C.W. Evans. Direct measurement of the redox potential of the primary and secondary quinone electron acceptors in *Rhodopseudomonas sphaeroides* (wild-type) by EPR spectrometry. *FEBS Letters*, 110(2):257–261, 1980.

[12] P.H. McPherson, M.Y. Okamura, and G. Feher. Electron transfer from the reaction center of *Rb. sphaeroides* to the quinone pool: doubly reduced Q_b leaves the reaction center. *Biochimica et Biophysica Acta - Bioenergetics*, 1016:289–292, 1990.

[13] R.K. Clayton. *Photosynthesis: Physical Mechanisms and Chemical Patterns*. Cambridge University Press, Cambridge, 1980.

[14] S. Malkin. Delayed luminescence. In J. Barber, editor, *Primary Processes of Photosynthesis*, pages 349–431. Elsevier, North-Holland Biomedical Press, 1977.

[15] H. Arata and W.W. Parson. Delayed fluorescence from *Rhodopseudomonas sphaeroides* reaction centers enthalpy and free energy changes accompanying electron transfer from P-870 to quinones. *Biochimica et Biophysica Acta - Bioenergetics*, 638:201–209, 1981.

[16] M.H. Stowell, T.M.McPhillips, D.C. Rees, S.M. Soltis, E. Abresch, and G.Fehér. Light-induced structural changes in photosynthetic reaction center: Implications for mechanism of electron-proton transfer. *Sciences*, 276(5313):812–816, 1997.

[17] P. Maróti and C.A. Wraight. Flash-induced H^+ binding by bacterial photosynthetic reaction centers: comparison of spectrophotometric and conductometric methods. *Biochimica et Biophysica Acta - Bioenergetics*, 934(3):314–328, 1988.

[18] K. Turzó, G. Laczkó, and P. Maróti. Delayed fluoreszcence study on $P^*Q_A \rightarrow P^+Q_A^-$ charge separation energetics linked to protons and salt in reaction centers from *Rhodobacter sphaeroides*. *Photosynthesis Research*, 55:235–240, 1998.

[19] S.J. Strickler and R.A. Berg. Relationship between absorption intensity and fluorescence lifetime of molecules. *J. Chem. Phys.*, 37:814–822, 1962.

[20] W.L. DeLano. *The PyMOL Molecular Graphics System*. DeLano Scientific, Palo Alto, CA, USA, 2002.

[21] J.P.P. Stewart. *MOPAC 93.00 Manual (Rev. 2)*. Fujitsu Limited, Tokyom Japan, 1993.

[22] J. Marelius, K. Kolmodin, I. Feierberg, and J. $\mathring{A}$qvist. Q: A molecular dynamics program for free energy calculations and empirical valence bond simulations in biomolecular systems. *Journal of Molecular Graphics and Modelling*, 16:213–225, 1998.

[23] G.M Moris, D.S. Goodsell, R.S. Halliday, R. Huey, W.E. Hart, R.K. Belew, and A.J. Olson. Automated docking using a lamarckian genetic algorithm and empirical binding free energy function. *Journal of Computional Chemistry*, 19:1639–1662, 1998.

[24] M.R. Gunner, D.E. Robertson, and P.L. Dutton. Kinetic studies on the reaction centers protein from *Rhodopseudomonas sphaeroides*: the temperature and free energy dependence of electron transfer between various quinones in the Q_A site and the oxidized bacteriochlorophyll dimer. *J. Phys. Chem. B*, 90:3783–3795, 1986.

[25] C.A. Wraight. Electron acceptors of bacterial photosythetic reaction centers: II. H^+ binding coupled to secondary electron transfer in the quinone acceptor complex. *Biochimica et Biophysica Acta - Bioenergetics*, 548:309–327, 1979.

[26] C.A. Wraight and R.R. Stein. Bacterial reaction centers as a model for photosystem ii. Turnover of the secondary acceptor quinone. In Y. Inoue, A.R. Crofts, N.M. Govindjee, G. Renger, and K. Satoh, editors, *The Oxigen Evolving System of Photosythesis*, pages 383–392. Academic Press, Tokyo, 1983.

[27] D. Kleinfeld, M.Y. Okamura, and G. Fehér. Electron transfer in reaction centers of *Rhodopseudomonas sphaeroides*. Determination of the charge recombination pathway of $D^+Q_aQ_b^-$ and free energy and kinetic relations between $Q_a^-Q_b$ and $Q_aQ_b^-$. *Biochimica et Biophysica Acta - Bioenergetics*, 766:126–140, 1984.

[28] K. Warncke, M.R. Gunner, B.S. Braun, L. Gu, C.A. Yu, J.M. Bruce, and P.L. Dutton. Influence of hydrocarbon tail structure on quinone binding and electron-transfer performance at the Q_A and Q_B sites of the photosynthetic reaction center protein. *Biochemistry*, 33:7830–7841, 1994.

[29] Z. Zhu and M.R. Gunner. Energetics of quinone-dependent electron and proton transfer in *Rhodobacter sphaeroides* photosynthetic reaction centers. *Biochemistry*, 44:82–96, 2005.

5. List of publications

I. **Rinyu L.**, Nagy L. and Körtvélyesi T.: The role of the electronic structure of quinones in the charge stabilization in photosynthetic reaction centers. Journal of Molecular Structure (Theochem), 571: 163-170, (2001).

II. **Rinyu L.**, Martin E.W., Takahashi E., Maróti P. and Wraight C.A.: Modulation of the free energy of the primary quinone acceptor (Q_A) in reaction centers from *Rhodobacter sphaeroides*: contributions from the protein and protein-lipid(cardiolipin) interactions. Biochimica et Biophysica Acta - Bioenergetics, 1655: 93-101, (2004).

III. Gerencsér L., **Rinyu L.**, Kálmán L., Takahashi E., Wraight C.A. and Maróti P.: Competitive binding of quinone and antibiotic stigmatellin to reaction centers of photosynthetic bacteria. Acta Biologica Szegediensis, 48(1-4): 25-33, (2004).

IV. **Rinyu L.**, Körtvélyesi T. and Maróti P.:Molecular dynamics approach to energetics of primary quinone in bacterial reaction centers. Manuscript (prepare for submission).

V. **Rinyu L.**, Méray N., Tandori J., Pfeiffer I., Maróti P., Nagy L.: Steric and electrostatic effects on the stabilization of the secondary quinone in reaction centers. Photosynthesis: Mechanism and effects. Proceedings of 11^{th} International Congress on Photosynthesis. Budapest, Hungary, 17-22 Aug., 1998. Szerk.: G. Garab. Dordrecht, Kluwer Academic Publishers, 833-, (1998).

VI. Nagy L., Fodor E., Tandori J., **Rinyu L.**, Farkas T.: Lipids affect the charge stabilization in wild-type and mutant reaction centers of *Rhodobacter sphaeroides* R-26. *Australian Journal of Plant Physiology* 26: 465- , (1999).

VII. Halmschlager A., Tandori J., Trotta M., **Rinyu L.**, Pfeiffer I., Nagy L.: A mathematical model for quinone-herbicide competition in the reaction centres of *Rhodobacter sphaeroides*. *Functional Plant Biology* 29: 433-, (2002).

VIII. Molnár M., Joó K., Barczi A., Szántó Zs., Futó I., Palcsu L., **Rinyu L.**: Dating of total soil organic matter used in kurgan studies. *Radiocarbon* 46: 413-, (2004).

IX. Molnár M., Szántó Zs., Svingor É., Palcsu L., Futó I., **Rinyu L.**: Gas generation measurements in drums containing LL/ILW. Waste Management, Energy Security and a Clean Environment. WM 04 Conference. Tucson, Arizona, Feb. 29 - March 4, 2004. Proceedings. Tucson, WM Symphosia Inc. 0: 204-, (2004).

X. Palcsu L., Svingor É., Szántó Zs., Molnár M., Futó I., Major Z., **Rinyu L.**: Isotopic composition of precipitation in Hungary in 2001 and 2002. International Symposium on Isotope Hydrology and Integrated Water Resources Management. Vienna, Austria, 19-23 May, 2004. Proceedings. Vienna, IAEA 0: 306-, (2004).

XI. Molnár M., Palcsu L., Svingor É., Futó I., Major Z., **Rinyu L.**, Veres M.: Isotope-analytical results of a study of gas generation in L/ILW. *Czechoslovak Journal of Physics* 56: 637-, (2006).

XII. Szántó Zs., Svingor É., Futó I., Palcsu L., Molnár M., **Rinyu L.**: A hydrochemical and isotopic case study around a near surface radioactive waste disposal. *Radiochimica Acta* 95: 55-, (2007).

XIII. **Rinyu L.**, Futó I., Kiss Á.Z., Molnár M., Svingor É., Quarta G., Calcagnile L.: Performance test of a new graphite target production facility in ATOMKI. *Radiocarbon*, manuscript accepted. (2007).

6. Chapter of book

Svingor É., Molnár M., Palcsu L., Futó I., Major Z., **Rinyu L.**, Szántó Zs., Barnabás I.: Monitoring vizsgálatok a Püspökszilágyi radioaktív hulladék kezelő és tároló környezetében. (in Hung.) Magyarország környezetkémiai állapota. Szerk.: Szendrei G. Bp., Innova Print Kft 161-, (2006).